Journal of Magnetism and Magnetic Materials 427 (2017) 85–89

Contents lists available at ScienceDirect

Journal of Magnetism and Magnetic Materials

journal homepage: www.elsevier.com/locate/jmmm

The force analysis for superparamagnetic nanoparticles-based gene delivery in an oscillating magnetic field

Jiajia Sun[a], Zongqian Shi[a,*], Shenli Jia[a], Pengbo Zhang[b]

[a] State Key Laboratory of Electrical Insulation and Power Equipment, Xi'an Jiaotong University, No. 28 Xianning West Road, Xi'an, Shaanxi Province 710049, China

[b] Department of Anesthesiology, Second Affiliated Hospital of Xi'an Jiaotong University School of Medicine, No.157 West 5 Road, Xi'an, Shaanxi Province 710004, China

ARTICLE INFO

Keywords:
Superparamagnetic nanoparticles
Oscillating magnetic field
Kelvin force
Cell
Magnetofection
Gene delivery

ABSTRACT

Due to the peculiar magnetic properties and the ability to function in cell-level biological interaction, superparamagnetic nanoparticles (SMNP) have been being the attractive carrier for gene delivery. The superparamagnetic nanoparticles with surface-bound gene vector can be attracted to the surface of cells by the Kelvin force provided by external magnetic field. In this article, the influence of the oscillating magnetic field on the characteristics of magnetofection is studied in terms of the magnetophoretic velocity. The magnetic field of a cylindrical permanent magnet is calculated by equivalent current source (ECS) method, and the Kelvin force is derived by using the effective moment method. The results show that the static magnetic field accelerates the sedimentation of the particles, and drives the particles inward towards the axis of the magnet. Based on the investigation of the magnetophoretic velocity of the particle under horizontally oscillating magnetic field, an oscillating velocity within the amplitude of the magnet oscillation is observed. Furthermore, simulation results indicate that the oscillating amplitude plays an important role in regulating the active region, where the particles may present oscillating motion. The analysis of the magnetophoretic velocity gives us an insight into the physical mechanism of the magnetofection. It's also helpful to the optimal design of the magnetofection system.

1. Introduction

Magnetofection, which is known as magnetic particles-based gene delivery under the influence of magnetic field [1], is a physical and non-viral delivery method, enhancing the transfection efficiency [2]. In the past decades, abundant investigations have been carried out to study the method for improving the magnetofection efficiency and the mechanism of particles uptake.

A static magnetic field can drive magnetic nanoparticles to move towards the magnetic source, which strengthens particle-cell interaction [3]. The work of Huth et al. established that the enhanced magnetofection efficiency in the presence of static magnetic field was due to the substantial sedimentation of SMNP instead of altering the cellular uptake mechanism of the particles [4]. They also denoted that the SMNP entered into the cells via clathrin-dependent as well as caveolae-mediated endocytic pathway, which was unrelated with the existence of magnetic field. These results were consistent with that of Lim et al. [5], who also investigated the influence of the oscillating magnetic array on the delivering process of short interfering ribonucleic acid-complexed magnetic nanoparticles.

The use of a combination of translational magnetic forces acting on the particles along *z*-axial and oscillation of the magnet array in the *x*-*y* plane was shown to be able to improve the magnetofection efficiency as compared with that of static array [5,6]. The oscillating magnet array promotes the particles moving across the cell surface with continuous mechanical stimulation, whereas, it does not change the mechanism of the cellular uptake.

Besides, McBain et al. carried out enormous experiments to investigate the influence of the oscillating frequency and amplitude of the magnet on magnetofection efficiency in human airway epithelial cells [7]. They obtained the best magnetofection efficiency when the frequency and amplitude of the oscillating magnet were 2 Hz and 200μm, respectively. Even though substantially experimental achievements have been obtained, it is still essential to investigate the physical mechanism underlying magnetofection.

The amplitude and gradient of magnetic field, which decide the Kelvin force, play a significant role in affecting transfection time and efficiency [6]. Besides, they also affect the magnetophoretic velocity of

* Corresponding author.
E-mail address: zqshi@mail.xjtu.edu.cn (Z. Shi).

http://dx.doi.org/10.1016/j.jmmm.2016.11.018
Received 22 June 2016; Received in revised form 25 October 2016; Accepted 1 November 2016
Available online 05 November 2016
0304-8853/

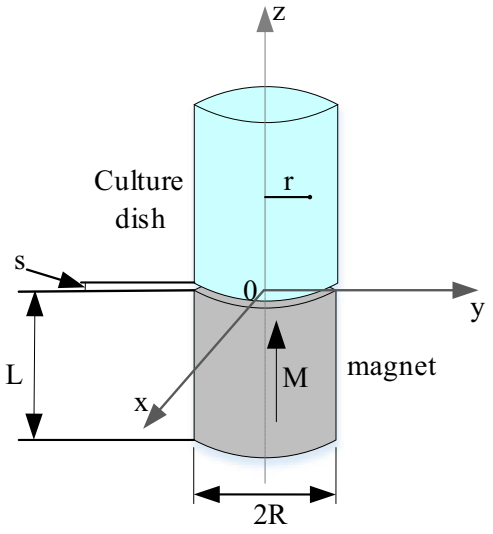

Fig. 1. The schematic diagram of cylindrical permanent magnet.

MNPs, which is defined as the steady-state moving velocity of particles [8]. Thus, in this study, at first, the magnetic field and Kelvin force generated by a static cylindrical permanent magnet is studied. Furthermore, the magnetophoretic velocity of the SMNP in the presence of an oscillating cylindrical permanent magnet is investigated. Finally, the influence of the oscillating amplitude of the magnet on the distribution of the magnetophoretic velocity is also analyzed.

2. Theory

The motion of the SMNP in the presence of oscillating magnetic field is governed by some key factors, including the magnitude of magnetic field, the field gradient, and the oscillating frequency and amplitude of the magnet, etc. In the following analysis, the magnetic field of a cylindrical permanent magnet with radius R=3 mm, height L=8 mm and magnetization M=9.55×10^5 A/m is considered as shown in Fig. 1. The origin of the coordinate is located at the center of the top surface of the magnet. The coordinate of a magnetic nanoparticle can be indicated by r and z, respectively. The distance between the magnet and the culture is S.

The ECS method is adopted to calculate the distribution of the magnetic field. For a cylindrical permanent magnet with a uniform axial magnetization, its magnetic field is the same as that of a surface current that flows around the circumference of the cylinder. Discretizing this "equivalent" surface current into a finite set of current loop elements, the total field can be obtained by summing the field distribution from the individual elements [9]. The Eq. (1) is used to describe the magnetic flux density ($\boldsymbol{B}$) of cylindrical permanent magnet,

$$\boldsymbol{B} = B_r \boldsymbol{e}_r + B_z \boldsymbol{e}_z \tag{1}$$

where $\boldsymbol{e}_r$ and $\boldsymbol{e}_z$ is the unit vector in radial and axial direction, respectively. B_r and B_z is the radial and axial component of the magnetic flux density, which are given as follows derived based on the ECS method [10]

$$B_r = \frac{\mu_0 M}{2\pi} \times \int_{-L}^{0} \frac{z-z'}{r[(R+r)^2+(z-z')^2]^{1/2}} \cdot \left[\frac{R^2+r^2+(z-z')^2}{(R-r)^2+(z-z')^2} \cdot E(k) - K(k) \right] dz' \tag{2}$$

$$B_z = \frac{\mu_0 M}{2\pi} \times \int_{-L}^{0} \frac{1}{[(R+r)^2+(z-z')^2]^{1/2}} \cdot \left[\frac{R^2-r^2-(z-z')^2}{(R-r)^2+(z-z')^2} \cdot E(k) + K(k) \right] dz' \tag{3}$$

where

$$K(k) = \int_0^{\frac{\pi}{2}} \frac{1}{\sqrt{1-k^2\sin^2\Phi}} d\Phi \quad , \quad E(k) = \int_0^{\frac{\pi}{2}} \sqrt{1-k^2\sin^2\Phi}\, d\Phi \tag{4}$$

The non-uniform magnetic field results in a translational force on magnetic nanoparticle in a direction decided by the field gradient [11]. The Kelvin force on particles can be derived by effective moment method which regards SMNP as magnetic point dipoles. The force on the magnetic dipoles is given as [12]

$$\boldsymbol{F}_m = \mu_f V_P (\boldsymbol{m}_p \cdot \nabla) \boldsymbol{H} \tag{5}$$

where V_p is the volume of the particle, and $\boldsymbol{H}$ is the external magnetic field applied by cylindrical permanent magnet at the center of particle. A linear magnetization model with saturation is used to predict the magnetization $\boldsymbol{m}_p$ of the particle. Below saturation, the magnetization of the particle is a linear function of the local field of the particle, which can be written as [13]

$$\boldsymbol{m}_p = \chi_p \boldsymbol{H}_{in} \tag{6}$$

where χ_p is the susceptibility of the particle, and $\boldsymbol{H}_{in}$=$\boldsymbol{H}$-$\boldsymbol{H}_{demag}$, where $\boldsymbol{H}_{demag}$=$\boldsymbol{m}_p$/3 is the self-demagnetization field of the spherical particle. If the particle is suspended in magnetically linear fluid with susceptibility of χ_f and $|\chi_f| \ll 1$, the magnetization of particle is [13]

$$\boldsymbol{m}_p = \frac{3(\chi_p - \chi_f)}{3 + (\chi_p - \chi_f)} V_p \boldsymbol{H} \tag{7}$$

Considering the saturation of the particle, the magnetization can be rewritten as [12]

$$\boldsymbol{m}_p = f(H)\boldsymbol{H} \tag{8}$$

where

$$f(H) = \begin{cases} \frac{3(\chi_p-\chi_f)}{(\chi_p-\chi_f)+3} & H < \left(\frac{(\chi_p-\chi_f)+3}{3\chi_p}\right) M_{sp} \\ M_{sp}/H & H \geq \left(\frac{(\chi_p-\chi_f)+3}{3\chi_p}\right) M_{sp} \end{cases} \tag{9}$$

In this equation, the M_{sp} is the saturation magnetization of the particle. With the assumption that the fluid is nonmagnetic (μ_f=μ_0 and χ_f=0), the Kelvin force can be rewritten as

$$\boldsymbol{F}_m = F_{mr}\boldsymbol{e}_r + F_{mz}\boldsymbol{e}_z \tag{10}$$

where

$$F_{mr} = \frac{V_p}{\mu_0} f(H) \left[B_r \frac{\partial B_r}{\partial r} + B_z \frac{\partial B_r}{\partial z} \right] \tag{11}$$

$$F_{mz} = \frac{V_p}{\mu_0} f(H) \left[B_r \frac{\partial B_z}{\partial r} + B_z \frac{\partial B_z}{\partial z} \right] \tag{12}$$

In present work, the adopted parameters are as follows, the radius of particle R_p=100 nm [4], S=1 mm, η=0.001 N s/m^2, and M_{sp}=4.78×10^5 A/m. The materials of magnet and superparamagnetic nanoparticles are assumed to be NdFeB and Fe_3O_4, respectively. Besides, the magnetization model Eq. (13), which is consistent with (9) when $\chi_p \gg 1$, is adopted [14].

$$f(H) = \begin{cases} 3 & H < M_{sp}/3 \\ M_{sp}/H & H \geq M_{sp}/3 \end{cases} \tag{13}$$

As the particle concentration is sufficiently dilute (particle volume concentration $c \leq 0.1$) [13], the interparticle interaction can be neglected. Then the motion of the particle in a viscous fluid can be described by Newtonian law [11]:

$$m_p \frac{d\boldsymbol{v}_p}{dt} = \boldsymbol{F}_m + \boldsymbol{F}_{vis} \tag{14}$$

In this paper, the fluid is assumed to be stationary, so the viscous drag force on a spherical particle with radius R_p and velocity $\boldsymbol{v}_p$ is given as [10]

$$\boldsymbol{F}_{vis} = -6\pi\eta R_p \boldsymbol{v}_p \tag{15}$$

where η is the viscous of the fluid. From (14) and (15) we can get the solution of $\boldsymbol{v}_p$ as shown in (16), where $\boldsymbol{v}_0$ and $\boldsymbol{v}_t = \boldsymbol{F}_m/(6\pi\eta R_p)$ are the initial and terminal velocity of the particle, respectively, and $\tau = m_p/(6\pi\eta R_p)$ is the time constant [11]. For a particle with radius on the order of hundreds of nanometers in present model configurations, the time constant is on the order of nanosecond, which means that it is acceptable to neglect the acceleration term of (14).

$$\boldsymbol{v}_p = \boldsymbol{v}_t + (\boldsymbol{v}_0 - \boldsymbol{v}_t)\exp\left(-\frac{t}{\tau}\right) \tag{16}$$

Therefore, the magnetophoretic velocity of the particle, which is proportional to the Kelvin force as shown in Eq. (17), can be adopted as the representation of the behavior of the particle.

$$\boldsymbol{v}_p = \frac{\boldsymbol{F}_m}{6\pi\eta R_p} = v_r \boldsymbol{e}_r + v_z \boldsymbol{e}_z \tag{17}$$

3. Results and discussions

In the presence of a static magnet, the radial distribution of B_r and B_z at z=1 mm are calculated by ECS method and the finite element analysis (FEA) method with commercial software, Ansys. As shown in Fig. 2, the B_r increases with the increase of r and reaches its peak near the periphery of the magnet. However, the B_z decreases with the increase of r and has a maximum at the center of the magnet as we have investigated [15].

Besides, the comparison of the results derived from the ECS and FEA methods denotes that the ECS method is suitable to describe the distribution of the magnetic field of a cylindrical permanent magnet. This close-form magnetic analysis provides an exact prediction of the magnetic field. It should be noted that while some commercial devices can be used to measure the distribution of the magnetic field, the concerned spatial resolution is on the scale of hundreds of nanometers. Therefore, a diagnostic facility with very high precision is required in order to obtain a successive field solution. Moreover, accurate calculation of Kelvin force requires higher resolution of magnetic field measurement, since it depends not only on the magnitude but also on the gradient of the magnetic field. In this connection, the analytic solution of the magnetic field of a cylindrical permanent magnet based on ECS method overcomes these limitations, and is suitable for investigating the magnetophoretic velocity.

The magnetic flux density combined with its gradient influences the profile of Kelvin force. The radial and axial components of the force in the presence of static magnetic field are shown in Fig. 3. In Fig. 3(a), for a given z, the F_{mr} increases with the increase of the radius until it reaches its peak at the periphery of the magnet. Furthermore, the maximum of F_{mr} decreases with the increase of z. It should be noted that F_{mr} is negative. It implies that the particles experience an inward force dragging them towards the center of the magnet while they are attracted towards the bottom of the culture as indicated by the horizontal arrow.

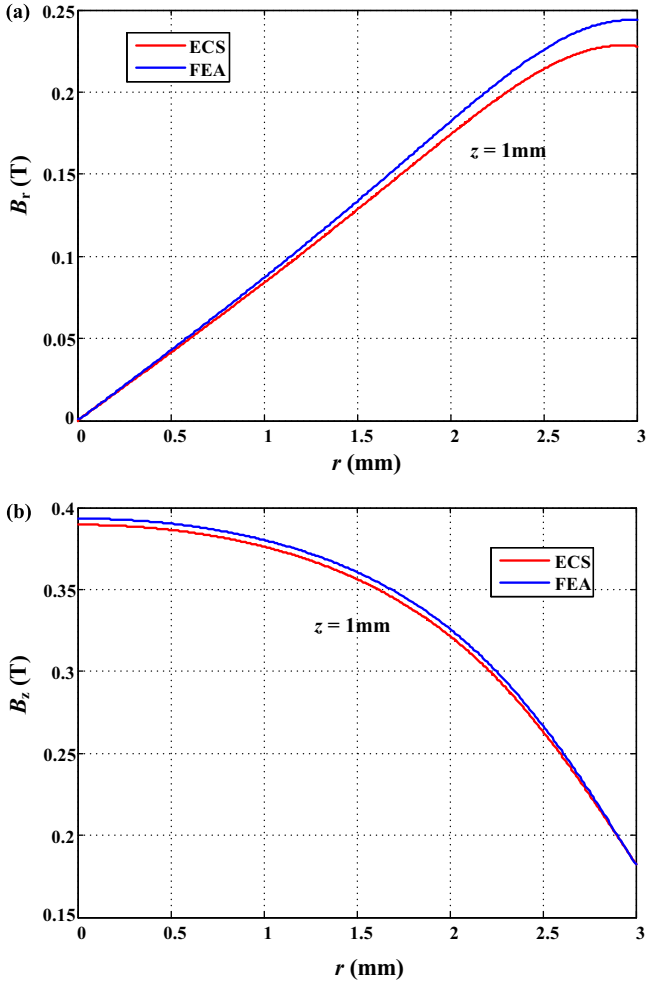

Fig. 2. The radial (a) and axial (b) component of static magnetic flux density at z=1 mm.

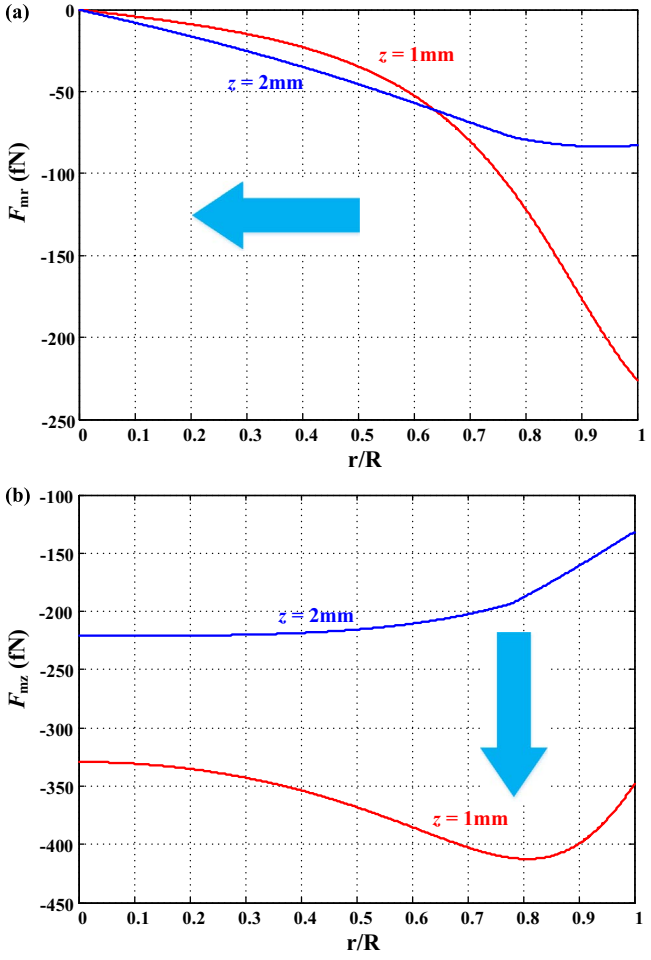

Fig. 3. The radial (a) and axial (b) component of Kelvin force in static magnetic field.

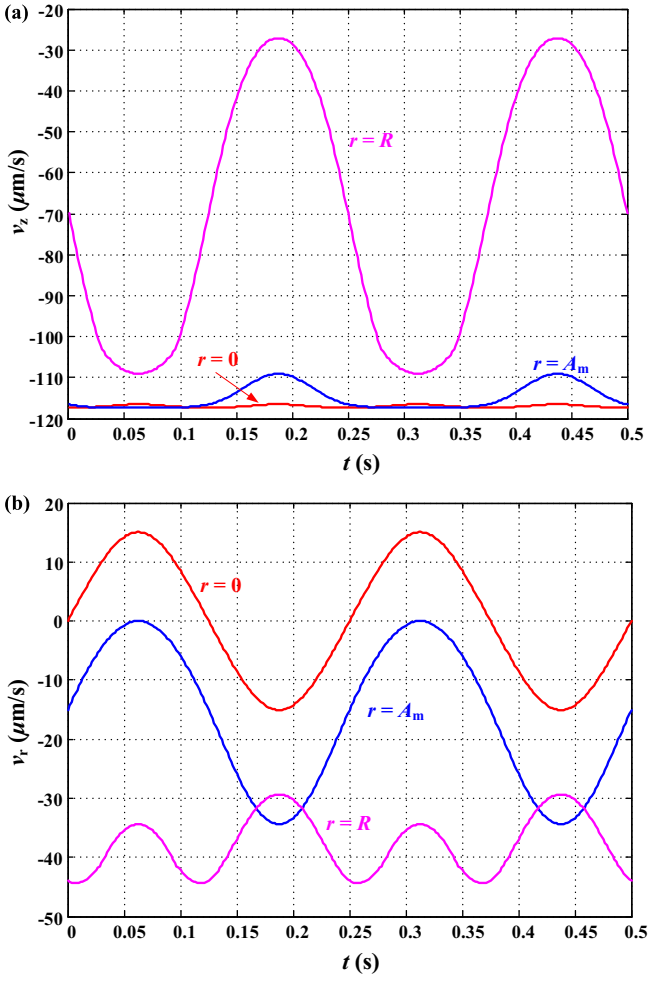

Fig. 4. The magnetophoretic velocity at three points r=0 mm, r=A_m, r=R with z=1 mm in the presence of oscillating magnetic field as a function of time with f=4 Hz and A_m=1 mm.

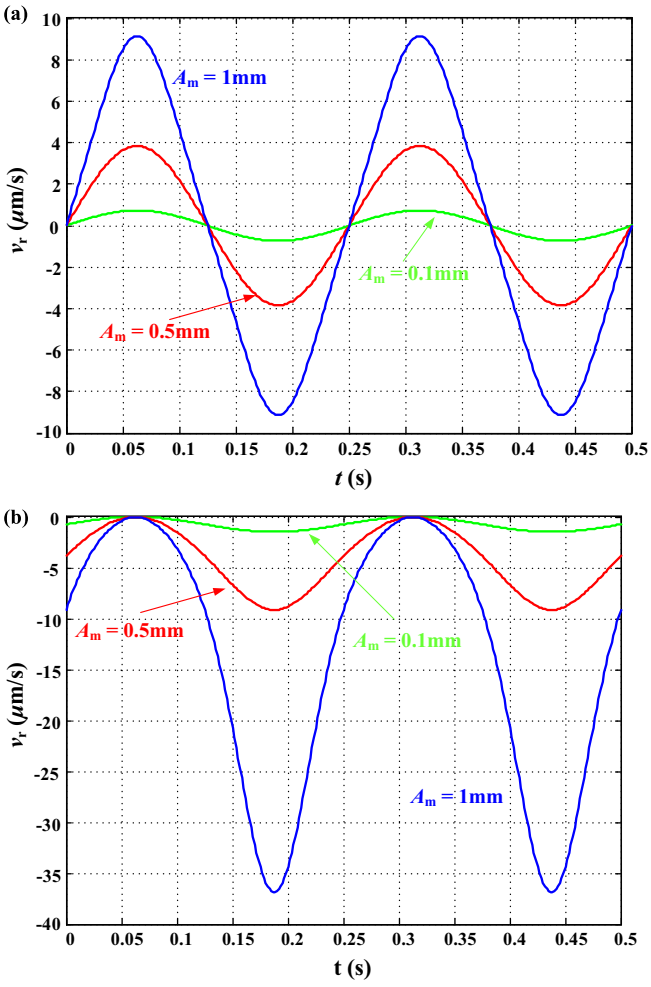

Fig. 5. The influence of the oscillating amplitude on the v_r at (a) r=0, z=1 mm and (b) r=A_m, z=1 mm with f=4 Hz as a function of time.

The results of Fig. 3(b) indicate that the amplitude of the F_{mz} at z=1 mm increases with the increase of r until it obtains maximum near the edge of the magnet, where it begins to decrease with further increase of r. First of all, it is the negative F_{mz} that accelerates the sedimentation of the particle. Furthermore, it can be seen from Fig. 3(b) that the amplitude of F_{mz} is always larger than F_{mr}, denoting that the particles near z=1 mm can be captured at the base of the culture close to their initial radial position. However, the F_{mz} at z=2 mm decreases with the increase of r. It means that particles, which are further away from the magnet, would be more likely to experience the attraction towards the center caused by the negative F_{mr}.

In the presence of oscillating magnetic field, the Eq. (18) is used to represent the coordinate (A) of the axis of the magnet along the y-axis.

$$A = A_m \sin(2\pi ft) \tag{18}$$

where A_m and f are the amplitude and frequency of the oscillation, respectively. Then the magnetophoretic velocity at three points, i.e., r=0, r=A_m, and r=R with z=1 mm, is simulated for two cycles with f=4 Hz and A_m=1 mm. As can be seen from Fig. 4(a), the v_z has a fluctuation near its initial value under the horizontal oscillating magnet. However, the fluctuation, which is dependent on the oscillating amplitude of the magnet, has a distinct difference among these three points. For example, the maximal fluctuation amplitude A_{vz} at r=R is nearly 40 μm/s, which is much higher than that at r=A_m with A_{vz}=5 μm/s and that at r=0 with A_{vz}≈0. This is caused by the difference of the radial gradient of the Kelvin force at different r, which can be deduced from the results of Fig. 3(b). Besides, the variation of the sedimentation velocity with time is more obvious for the particles near the periphery of the culture than that near the center of the culture.

In Fig. 4(b), the v_r at the point r=0 varies from positive to negative in one oscillating cycle. The amplitude of the oscillation (A_{vr}) is 15 μm/s, which implies that for the particles that pass through r=0, they may obtain different radial velocity at different time. It should be noted that the velocity changes in direction as well as in the amplitude. However, the variation of v_r at the point with r=A_m and r=R does not have any change in direction. It means that the particles within this region are always attracted towards the center of the culture without any oscillating motion. Furthermore, the profile of the v_r at r=A_m implies a critical oscillating region. For the particles in the region $r < A_m$, an alternation of negative or positive velocity v_r can impel the particles towards or outwards the center of the culture repeatedly, which results in an oscillating motion of the particles.

Above results indicate that the dynamics of magnetic nanoparticles is closely related with the oscillating amplitude of the magnet. Then the influence of the oscillating amplitude of the magnet on v_r (at r=0, r=A_m and z=1 mm) is investigated in Fig. 5 with f=4 Hz. The results of Fig. 5(a) show that the oscillating amplitude of the velocity A_{vr} increases with the increase of A_m, which indicates that the oscillating motion of the particles can be strengthened with the increase of the oscillating amplitude A_m. However, the v_r at r=A_m keeps negative all the time, which attracts the particles inward without any change in direction.

The different characteristics of the oscillation of v_r between r=0 and

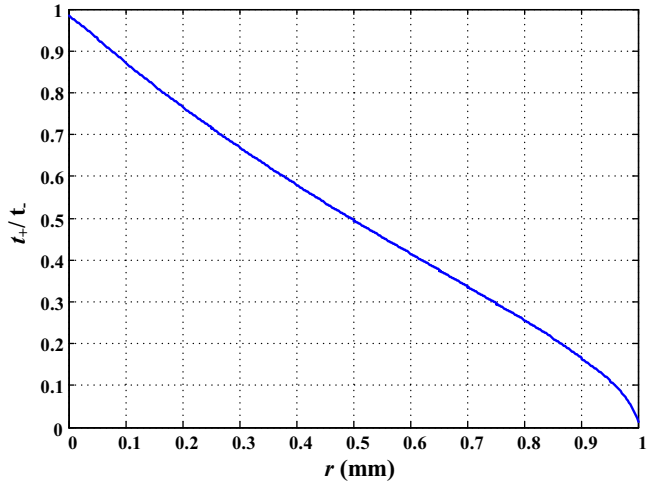

Fig. 6. t_+/t_- in the region $r < A_m$ with f=4 Hz and A_m=1 mm.

$r=A_m$ implies that the existence of particle oscillating motion is dependent on the relationship between the A_m and the coordinate r of particle. It indicates that only the particles at $r < A_m$ can present oscillating motion. Furthermore, this oscillating motion of particles is more obvious near the center than that close to the critical position $r=A_m$.

We can define the positive action time (t_+) and negative action time (t_-) as the duration of positive and negative radial velocity, respectively. The ratio of the positive and negative action time (t_+/t_-) at $r < A_m$ with f=4 Hz and A_m=1 mm is also investigated as shown in Fig. 6. It shows that the ratio decreases with the increase of the radial position r. Thus, the possibility that particles present oscillating behavior decreases with the increase of r.

4. Conclusion

In this article, the physical mechanism of the magnetofection in the presence of oscillating magnetic field is investigated via analyzing the magnetic field and the magnetophoretic velocity (proportional to the Kelvin force). Following conclusions can be drawn on this paper.

The results show that the static magnetic field accelerates the sedimentation of the particles, and drives the particles inward towards the axis of the magnet.

The oscillating cylindrical permanent magnet acts an oscillating radial Kelvin force on the particles in the region $r < A_m$. Thus, for the particles at this region, this oscillating force could lead to an oscillating motion to the particles in the radial direction. The horizontal oscillating motion of the particles can contribute to the enhanced magnetofection efficiency.

The simulation results also indicate that the oscillating amplitude plays an important role in regulating the active region, where the particles may present oscillating motion.

Acknowledgements

The work was supported in part by Fundamental Research Funds for the Central Universities, and in part by the National Natural Science Foundation of China under project 51322706 and 51325705.

References

[1] D. Ang, Q.V. Nguyen, S. Kayal, P.R. Preiser, R.S. Rawat, R.V. Ramanujan, Insights into the mechanism of magnetic particle assisted gene delivery, Acta Biomater. 7 (2011) 1319–1326.
[2] C. Plank, O. Zelphati, O. Mykhaylyk, Magnetically enhanced nucleic acid delivery. Ten years of magnetofection-progress and prospects, Adv. Drug Deliv. Rev. 63 (2011) 1300–1331.
[3] C.F. Adams, M.R. Pickard, D.M. Chari, Magnetic nanoparticle mediated transfection of neural stem cell suspension cultures is enhanced by applied oscillating Magnetic fields, Nanomed. Nanotechnol. Biol. Med. 9 (2013) 737–741.
[4] S. Huth, J. Lausier, S.W. Gersting, C. Rudolph, C. Plank, U. Welsch, J. Rosenecker, Insights into the mechanism of magnetofection using PEI-based magnetofectins for gene transfer, J. Gene Med. 6 (2004) 923–936.
[5] Michael A. Clements, J. Lim, J. Dobson, Delivery of short interfering ribonucleic acid-complexed magnetic nanoparticles in an oscillating field occurs via caveolae-mediated endocytosis, PloS One (2012).
[6] A. Fouriki, N. Farrow, M.A. Clements, J. Dobson, Evaluation of the magnetic field requirements for nanomagnetic gene transfection, Nano Rev. 1 (2010).
[7] S.C. McBain, U. Griesenbach, S. Xenariou, A. Keramane, C.D. Batich, E.W. Alton, J. Dobson, Magnetic nanoparticles as gene delivery agents: enhanced transfection in the presence of oscillating magnet arrays, Nanotechnology 19 (2008) 405102.
[8] J.S. Andreu, P. Barbero, J. Camacho, J. Faraudo, Simulation of magnetophoretic separation processes in dispersions of superparamagnetic nanoparticles in the noncooperative regime, J. Nanomater. 2012 (2012) 1–10.
[9] E.P. Furlani, Permanent magnet and electromechanical devices: materials, analysis, and applications, Academic press, 2001.
[10] E.P. Furlani, X. Xue, Field, force and transport analysis for magnetic particle-based gene delivery, Microfluid. Nanofluidics 13 (2012) 589–602.
[11] Q. Cao, X. Han, L. Li, Numerical analysis of magnetic nanoparticle transport in microfluidic systems under the influence of permanent magnets, J. Phys. D Appl. Phys. 45 (2012) 465001.
[12] E.P. Furlani, X. Xue, A model for predicting field-directed particle transport in the magnetofection process, Pharm. Res. 29 (2012) 1366–1379.
[13] E.P. Furlani, Analysis of particle transport in a magnetophoretic microsystem, J. Appl. Phys. 99 (2006) 024912.
[14] R. Gerber, M. Takayasu, F. Friedlaender, Generalization of HGMS theory: the capture of ultra-fine particles, Shock 19 (1983) 2115–2117.
[15] J.Sun, Z.Shi, J.Bai, S.Jia, P.Zhang, Numerical investigation on the magnetic field of cylindrical permanent magnet for magnetic nanoparticles application, in: Nanotechnology (IEEE-NANO), 2015 IEEE Proceedings of the 15th International Conference 2015, pp. 1041–1044.